

Visible Light-Driven Water Oxidation by a Molecular Ruthenium Catalyst in Homogeneous System

Lele Duan,[†] Yunhua Xu,[†] Pan Zhang,[‡] Mei Wang,[‡] and Licheng Sun^{*,†,‡}

[†]Department of Chemistry, School of Chemical Science and Engineering, Royal Institute of Technology (KTH), 100 44 Stockholm, Sweden and [‡]DUT-KTH Joint Education and Research Center on Molecular Devices, State Key Laboratory of Fine Chemicals, Dalian University of Technology (DUT), 116012, Dalian, China

Received September 2, 2009

Discovery of an efficient catalyst bearing low overpotential toward water oxidation is a key step for light-driven water splitting into dioxygen and dihydrogen. A mononuclear ruthenium complex, Ru(II)L(pic)₂ (**1**) (H₂L = 2,2'-bipyridine-6,6'-dicarboxylic acid; pic = 4-picoline), was found capable of oxidizing water electrochemically at a relatively low potential and promoting light-driven water oxidation using a three-component system composed of a photosensitizer, sacrificial electron acceptor, and complex **1**. The detailed electrochemical properties of **1** were studied, and the onset potentials of the electrochemically catalytic curves in pH 7.0 and pH 1.0 solutions are 1.0 and 1.5 V, respectively. The low catalytic potential of **1** under neutral conditions allows the use of [Ru(bpy)₃]²⁺ and even [Ru(dmbpy)₃]²⁺ as a photosensitizer for photochemical water oxidation. Two different sacrificial electron acceptors, [Co(NH₃)₅Cl]Cl₂ and Na₂S₂O₈, were used to generate the oxidized state of ruthenium tris(2,2'-bipyridyl) photosensitizers. In addition, a two-hour photolysis of **1** in a pH 7.0 phosphate buffer did not lead to obvious degradation, indicating the good photostability of our catalyst. However, under conditions of light-driven water oxidation, the catalyst deactivates quickly. In both solution and the solid state under aerobic conditions, complex **1** gradually decomposed via oxidative degradation of its ligands, and two of the decomposed products, sp³C–H bond oxidized Ru complexes, were identified. The capability of oxidizing the sp³C–H bond implies the presence of a highly oxidizing Ru species, which might also cause the final degradation of the catalyst.

Introduction

In nature, water is oxidized by the oxygen-evolving complex (OEC) in photosystem II (PSII) driven by light, providing electrons and protons for the sustainability of all life forms on earth. Inspired by the function of OEC, tremendous efforts have been made on artificial photosynthesis systems aiming at light-driven water splitting into molecular hydrogen and oxygen.^{1–5} This approach is extremely important for solar energy conversion into a fuel, and the ultimate challenge in this approach is the catalytic water oxidation driven by visible light.⁵ In heterogeneous systems, light-driven water oxidation or water splitting has been demonstrated in several ways, such as electrolysis using photovoltaic cells,⁶ semiconductor-based photoelectrodes via the photoinduced electron

and hole separation,^{7–10} and catalytic systems composed of transition-metal photosensitizers and metal (Ir and Ru) oxide water oxidation catalysts.^{11,12} On the other hand, light-driven water oxidation in homogeneous systems is rarely reported.

A few molecular complexes have been reported to catalyze the oxidation of water. Few Mn complexes {[terpy)₂Mn₂O₂-(H₂O)₂](NO₃)₃ (terpy = 2,2':6',2''-terpyridine),^{13,14} [Mn₂L^a₂-(H₂O)₂](ClO₄)₂ (L^a = N-methyl-N'-glycyl-N,N'-bis(2-pyridylmethyl)ethane-1,2-diamine; it should be noted that one oxygen atom in the generated dioxygen by this catalyst comes from oxidant),¹⁵ and L^b₆Mn₄O₄ cubanes (L^b = (p-R-C₆H₄)₂PO₂⁻,

*To whom correspondence should be addressed. E-mail: lichengs@kth.se.

(1) Alstrum-Acevedo, J. H.; Brennaman, M. K.; Meyer, T. J. *Inorg. Chem.* **2005**, *44*, 6802.
(2) Eisenberg, R.; Gray, H. *Inorg. Chem.* **2008**, *47*, 1697.
(3) Balzani, V.; Credi, A.; Venturi, M. *ChemSusChem* **2008**, *1*, 26.
(4) Sun, L.; Hammarström, L.; Akermark, B.; Stryring, S. *Chem. Soc. Rev.* **2001**, *30*, 36.
(5) Meyer, T. J. *Acc. Chem. Res.* **1989**, *22*, 163.
(6) Khaselev, O.; Turner, J. A. *Science* **1998**, *280*, 425.
(7) Khan, S. U. M.; Al-Shahry, M.; Ingler, W. B., Jr. *Science* **2002**, *297*, 2243.

(8) Zou, Z.; Ye, J.; Sayama, K.; Arakawa, H. *Nature* **2001**, *414*, 625.
(9) Zhong, D. K.; Sun, J.; Inumaru, H.; Gamelin, D. R. *J. Am. Chem. Soc.* **2009**, *131*, 6086.
(10) Kudo, A.; Kato, H.; Tsuji, I. *Chem. Lett.* **2004**, *33*, 1534.
(11) Kalyanasundaram, K.; Grätzel, M. *Angew. Chem., Int. Ed.* **1979**, *18*, 701.
(12) Youngblood, W. J.; Lee, S.-H. A.; Kobayashi, Y.; Hernandez-Pagan, E. A.; Hoertz, P. G.; Moore, T. A.; Moore, A. L.; Gust, D.; Mallouk, T. E. *J. Am. Chem. Soc.* **2009**, *131*, 926.
(13) Limburg, J.; Vrettos, J. S.; Liable-Sands, L. M.; Rheingold, A. L.; Crabtree, R. H.; Brudvig, G. W. *Science* **1999**, *283*, 1524.
(14) Yagi, M.; Narita, K. *J. Am. Chem. Soc.* **2004**, *126*, 8084.
(15) Poulsen, A. K.; Rompel, A.; McKenzie, C. J. *Angew. Chem., Int. Ed.* **2005**, *44*, 6916.

R = H, Me, OMe)}^{16,17} were described to be functional toward water oxidation with low to high turnover numbers (TONs). In contrast, many more ruthenium-based water oxidation catalysts were produced with promising catalytic properties. In the early 1980s, Meyer and co-workers reported an oxo-bridged dinuclear ruthenium complex, {*cis,cis*-[Ru(bpy)₂(H₂O)]₂(μ-O)⁴⁺} (bpy = 2,2'-bipyridine), the so-called "blue dimer", that efficiently catalyzes water oxidation.^{18,19} Since then, more and more efforts have been devoted to the design of more active ruthenium-based catalysts, and fruitful results have been obtained. Several derivatives of the "blue dimer" were synthesized with more or less enhanced catalytic activities.^{20–23} Kaneko and Yagi investigated a series of amine-coordinated Ru complexes, [(NH₃)₅Ru^{III}(μ-O)Ru^{IV}(NH₃)₄(μ-O)Ru^{III}(NH₃)₅]⁶⁺, for instance, as water oxidation catalysts in both homogeneous and heterogeneous systems.²⁴ Tanaka and co-workers reported a novel dinuclear Ru complex, [Ru₂(OH)₂(3,6-Bu₂Q)₂(btpyan)](SbF₆)₂ (3,6-Bu₂Q = 3,6-di-*tert*-butyl-1,2-benzoquinone; btpyan = 1,8-bis-(2,2':6',2''-terpyrid-4'-yl)anthracene), with redox-active quinone ligands.²⁵ In 2004, Llobet et al. reported a dinuclear Ru complex, {[Ru(II)(terpy)(H₂O)]₂(μ-bpp)}³⁺ (bpp = 2,6-bis(pyridyl)pyrazolate), using bpp as a bridging ligand instead of an oxo bridge, and a turnover number of 34 toward water oxidation using Ce(IV) as an oxidant at pH 1.0 was achieved.²⁶ After ligand modification, this type of Ru-bpp-based water oxidation catalyst was anchored on conducting solid supports, and a TON of 250 was achieved in the heterogeneous phase using Ce(IV) as an oxidant.²⁷ Recently, several mononuclear ruthenium aqua complexes containing terpyridine as the backbone and only one aqua ligand in each complex were reported active toward water oxidation, and the reaction kinetics are first order with respect to catalysts.^{28,29} Meyer and co-workers proposed a seven-coordinate ruthenium intermediate during the catalytic processes.²⁸ Thummel and co-workers developed a series of non-aqueous polypyridyl ruthenium complexes that catalyze water

oxidation with higher reactivity.^{30–33} Notably, to demonstrate the mechanistic aspect, one of the mononuclear non-aqua ruthenium complexes was studied in detail, and this catalyst could be recovered without ligand exchange after several catalytic cycles. Consequently, a plausible mechanism involving seven-coordinate ruthenium species was also proposed.³⁰ To avoid using organic ligands in the construction of water oxidation catalysts, Hill, Bonchio, and their co-workers developed a new purely inorganic water-soluble catalyst, a Ru polyoxometalate [{Ru₄O₄(OH)₂(H₂O)₄}(γ-SiW₁₀O₃₆)₂]¹⁰⁻.^{34,35} In addition to ruthenium-based complexes, robust Ir catalysts capable of catalyzing water oxidation with low reaction rates have been reported by Bernhard and co-workers.³⁶ On the basis of this work, Crabtree and co-workers designed several Cp*-based iridium complexes and gained an increase in the reaction rate and a decrease in the robustness.³⁷

For photoinduced water oxidation in homogeneous systems, the functional catalysts are few. In principle, photosensitizers with oxidation potentials higher than 0.82 V are able to drive water oxidation, since the oxidation of water to molecular oxygen thermodynamically happens at 0.82 V versus NHE under pH 7.0 conditions. However, to the best of our knowledge, among the rare water oxidation catalysts, only a couple of dimeric ruthenium complexes,^{23,38,39} a tetra-ruthenium polyoxometalate complex,⁴⁰ and CoSO₄⁴¹ were reported to promote photochemical water oxidation in homogeneous systems in the presence of photosensitizers [Ru(bpy)₃]²⁺ or Ru(4,4'-DCE-bpy)₃²⁺ (4,4'-DCE-bpy = 4,4'-dicarboxyethyl-2,2'-bipyridine). Another Ru(II) complex has been reported to split water stoichiometrically into dihydrogen and dioxygen in consecutive thermal- and light-driven steps.⁴²

Aiming at light-driven water oxidation (Scheme 1), we attempted to lower the oxidation potential of ruthenium-based water oxidation catalysts by introducing negatively charged ligands and to match the redox potential of [Ru(bpy)₃]²⁺, which is a well-known photosensitizer with good photophysical properties and a long lifetime of its excited state. We have reported a dinuclear ruthenium complex with a negatively charged ligand which greatly lowers the oxidation potential of the ruthenium complex.⁴³ Benefiting from the stabilization of the high valent ruthenium complex by a negatively charged ligand, very recently, we have designed a mononuclear ruthenium complex, Ru(II)L(pic)₂ (**1**) (see the structure in Scheme 1; H₂L = 2,2'-bipyridine-6,6'-dicarboxylic

(16) Yagi, M.; Wolf, K. V.; Baesjou, P. J.; Bernasek, S. L.; Dismukes, G. C. *Angew. Chem., Int. Ed.* **2001**, *40*, 2925.

(17) Brimblecombe, R.; Swiegers, G. F.; Dismukes, G. C.; Spiccia, L. *Angew. Chem., Int. Ed.* **2008**, *47*, 7335.

(18) Gersten, S. W.; Samuels, G. J.; Meyer, T. J. *J. Am. Chem. Soc.* **1982**, *104*, 4029.

(19) Gilbert, J. A.; Eggleston, D. S.; Murphy, W. R.; Geselowitz, D. A.; Gersten, S. W.; Hodgson, D. J.; Meyer, T. J. *J. Am. Chem. Soc.* **1985**, *107*, 3855.

(20) Petach, H. H.; Elliot, M. J. *Electrochem. Soc.* **1992**, *139*, 2217.

(21) Lai, Y. K.; Wong, K. Y. *J. Electroanal. Chem.* **1995**, *380*, 193.

(22) Nazeeruddin, M. K.; Rotzinger, F. P.; Comte, P.; Grätzel, M. *J. Chem. Soc., Chem. Commun.* **1988**, 872.

(23) Rotzinger, F. P.; Munavalli, S.; Comte, P.; Hurst, J. K.; Grätzel, M.; Pern, F. J.; Frank, A. J. *J. Am. Chem. Soc.* **1987**, *109*, 6619.

(24) Yagi, M.; Kaneko, M. *Chem. Rev.* **2000**, *101*, 21.

(25) (a) Wada, T.; Tsuge, K.; Tanaka, K. *Inorg. Chem.* **2000**, *40*, 329. (b) Muckerman, J. T.; Polyansky, D. E.; Wada, T.; Tanaka, K.; Fujita, E. *Inorg. Chem.* **2008**, *47*, 1787.

(26) Sens, C.; Romero, I.; Rodriguez, M.; Llobet, A.; Parella, T.; Benet-Buchholz, J. J. *Am. Chem. Soc.* **2004**, *126*, 7798.

(27) Mola, J.; Mas-Marza, E.; Sala, X.; Romero, I.; Rodriguez, M.; Viñas, C.; Parella, T.; Llobet, A. *Angew. Chem., Int. Ed.* **2008**, *47*, 5830.

(28) Concepcion, J. J.; Jurss, J. W.; Templeton, J. L.; Meyer, T. J. *J. Am. Chem. Soc.* **2008**, *130*, 16462.

(29) (a) Yoshida, M.; Masaoka, S.; Sakai, K. *Chem. Lett.* **2009**, *38*, 702. (b) Masaoka, S.; Sakai, K. *Chem. Lett.* **2009**, *38*, 182.

(30) Tseng, H.-W.; Zong, R.; Muckerman, J. T.; Thummel, R. *Inorg. Chem.* **2008**, *47*, 11763.

(31) Deng, Z.; Tseng, H.-W.; Zong, R.; Wang, D.; Thummel, R. *Inorg. Chem.* **2008**, *47*, 1835.

(32) Zhang, G.; Zong, R.; Tseng, H.-W.; Thummel, R. P. *Inorg. Chem.* **2008**, *47*, 990.

(33) Zong, R.; Thummel, R. P. *J. Am. Chem. Soc.* **2005**, *127*, 12802.

(34) Geletii, Y. V.; Botar, B.; Köerler, P.; Hillesheim, D. A.; Musaev, D. G.; Hill, C. L. *Angew. Chem., Int. Ed.* **2008**, *120*, 3960.

(35) Sartorel, A.; Carraro, M.; Scorrano, G.; Zorzi, R. D.; Geremia, S.; McDaniel, N. D.; Bernhard, S.; Bonchio, M. *J. Am. Chem. Soc.* **2008**, *130*, 5006.

(36) McDaniel, N. D.; Coughlin, F. J.; Tinker, L. L.; Bernhard, S. *J. Am. Chem. Soc.* **2008**, *130*, 210.

(37) Hull, J. F.; Balcells, D.; Blakemore, J. D.; Incarvito, C. D.; Eisenstein, O.; Brudvig, G. W.; Crabtree, R. H. *J. Am. Chem. Soc.* **2009**, *131*, 8730.

(38) Cape, J. L.; Hurst, J. K. *J. Am. Chem. Soc.* **2008**, *130*, 827.

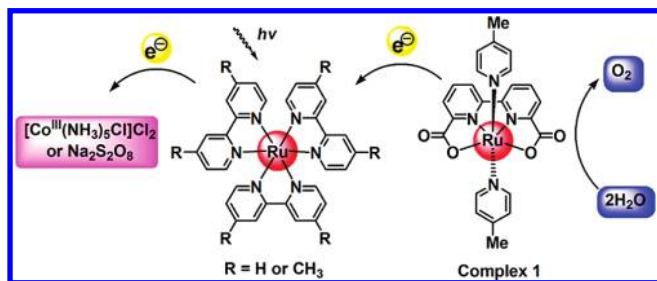
(39) Comte, P.; Nazeeruddin, M. K.; Rotzinger, F. P.; Frank, A. J.; Grätzel, M. *J. Mol. Catal.* **1989**, *52*, 63.

(40) Geletii, Y. V.; Huang, Z.; Hou, Y.; Musaev, D. G.; Lian, T.; Hill, C. L. *J. Am. Chem. Soc.* **2009**, *131*, 7522.

(41) Harriman, A.; Porter, G.; Walters, P. J. *Chem. Soc., Faraday Trans. 2* **1981**, *77*, 2373.

(42) Kohl, S. W.; Weiner, L.; Schwartsburd, L.; Konstantinovskii, L.; Shimon, L. J. W.; Ben-David, Y.; Iron, M. A.; Milstein, D. *Science* **2009**, *324*, 74.

(43) Xu, Y.; Åkermark, T.; Gyollai, V.; Zou, D.; Eriksson, L.; Duan, L.; Zhang, R.; Åkermark, B.; Sun, L. *Inorg. Chem.* **2009**, *48*, 2717.

Scheme 1. Visible Light-Driven Water Oxidation Using Three-Component Molecular Systems

acid; pic = 4-picoline), with a dicarboxylate ligand as an efficient water oxidation catalyst, and a seven-coordinate Ru(IV) intermediate has been successfully isolated and structurally characterized.⁴⁴

In particular, complex **1** was found to be capable of catalyzing water oxidation at low overpotentials. Herein, we report the electrochemical properties of complex **1** in water, and the visible light-driven water oxidation by complex **1** using photosensitizers of $[\text{Ru}(\text{bpy})_3]^{2+}$ ($E_{1/2} = 1.26$ V) and even $[\text{Ru}(\text{dmbpy})_3]^{2+}$ ($E_{1/2} = 1.10$ V; dmbpy = 4,4'-dimethyl-2,2'-bipyridine; Scheme 1).

Experimental Section

General Considerations. Complex **1**, $[\text{Ru}(\text{dmbpy})_3](\text{PF}_6)_2$, and $[\text{Ru}(\text{bpy})_3](\text{PF}_6)_3$ were prepared according to the literature methods.^{44–46} $[\text{Ru}(\text{bpy})_3]\text{Cl}_2 \cdot 6\text{H}_2\text{O}$, $\text{RuCl}_3 \cdot x\text{H}_2\text{O}$, 4,4'-dimethyl-2,2'-bipyridine, sodium persulfate, a pH 7.0 phosphate buffer (50 mM), and a pH 7.2 phosphate buffer (8.3 mM) were purchased from Aldrich, and all other chemicals are commercially available. At room temperature, the concentration of the saturated $[\text{Co}(\text{NH}_3)_5\text{Cl}]\text{Cl}_2$ in a phosphate buffer (initial pH 7.0, 50 mM) was quantitatively analyzed to be 29 mM with UV–vis spectrometry. The NMR spectra were recorded with a 400 MHz of Bruker Avance spectrometer. Mass spectrometry measurements were performed on a Q-ToF Micro mass spectrometer. UV–vis absorption spectra were measured with a PerkinElmer Lambda 750 UV–vis spectrophotometer. Cyclic voltammetric (CV) measurements were carried out with an Autolab potentiostat with a GPES electrochemical interface (Eco Chemie), using a glassy carbon disk (diameter 3 mm) as the working electrode, a platinum spiral in a compartment separated from the bulk solution by a fritted disk as the counter-electrode, and an Ag/AgCl electrode (3 M KCl aqueous solution) as the reference electrode. The cyclic voltammograms were obtained in either a phosphate buffer (pH 7.0) solution or a $\text{CF}_3\text{SO}_3\text{H}$ aqueous solution (pH 1.0) containing 10% acetonitrile.

Irradiation and Photolysis. The photochemical oxygen evolution was investigated under irradiation with a 500 W xenon arc lamp equipped with a 400 nm cutoff filter and a water jacket to remove UV and IR radiation, respectively. The intensity where irradiated is ~ 0.3 W/cm². The photolysis of a complex **1** aqueous solution (5×10^{-5} M) in a phosphate buffer (pH 7.0) containing 5% acetonitrile was studied using the above-mentioned light source. The deoxygenated solution was irradiated under stirring and cooled with a water cooling system. The absorption spectra of the solution were monitored by a PerkinElmer Lambda 750 UV–vis spectrophotometer.

Oxygen Evolution. The oxygen evolution was analyzed with either a Clark-type oxygen electrode (Hansatech Instruments,

DW2/2 unit with an S1 electrode; more details of the S1 electrode and DW2/2 unit could be obtained from the Web site of Hansatech Instruments Ltd.) or GC chromatography (a GC 7890T instrument with a thermal conductivity detector, a 5 Å molecular sieve column, and with Ar as the carrying gas).

1. Oxygen Evolution Monitored by Oxygen Electrode. Oxygen evolution by complex **1** using $[\text{Ru}(\text{bpy})_3](\text{PF}_6)_3$ as the oxidant was recorded with an oxygen electrode. A degassed acetonitrile solution of **1** (100 μL , 80 μM , 8 nmol) was injected using a syringe through a septum into 2 mL of a deoxygenated phosphate buffer (pH 7.0) solution containing a small amount of $[\text{Ru}(\text{bpy})_3](\text{PF}_6)_3$ (due to the instability of $[\text{Ru}(\text{bpy})_3](\text{PF}_6)_3$ under neutral conditions, we used it directly without drying; therefore, the exact amount of this oxidant was uncertain). The generated O_2 was measured and recorded versus time (Figure S1, Supporting Information).

For photochemical oxygen generation, the reaction system was cooled by a circulated water cooling system. Generally, for the three-component system, the catalyst, sensitizer, and electron acceptor were dissolved in a phosphate buffer solution (total 2 mL). After degassing, the above solution was irradiated and the formation of oxygen was recorded by oxygen electrode. The other control experiments were carried out in a similar way. For the $[\text{Co}(\text{NH}_3)_5\text{Cl}]^{2+}$ system, the concentrations of **1**, the photosensitizer ($[\text{Ru}(\text{bpy})_3]^{2+}$ or $[\text{Ru}(\text{dmbpy})_3]^{2+}$), and $[\text{Co}(\text{NH}_3)_5\text{Cl}]^{2+}$ were 5.5×10^{-6} M, 6.7×10^{-5} M, and 2.9×10^{-2} M, respectively. In the $\text{S}_2\text{O}_8^{2-}$ system, the concentrations of complex **1**, $[\text{Ru}(\text{bpy})_3]^{2+}$, and $\text{S}_2\text{O}_8^{2-}$ were 9.5×10^{-6} M, 1×10^{-3} M, and 1×10^{-2} M, respectively.

2. Oxygen Evolution Monitored by GC. In a typical experiment, $[\text{Co}(\text{NH}_3)_5\text{Cl}]\text{Cl}_2$ (36.2 mg, 1.45 μmol), $[\text{Ru}(\text{bpy})_3]\text{Cl}_2$ (25 μL , 2 mM), complex **1** (100 μL , 0.5 mM), and a pH 7.0 phosphate buffer (5 mL) were added to a Schlenk tube. The solution was degassed using the freeze–pump technique three times and then warmed to room temperature prior to irradiation. The total volume (containing the gas phase and the solution) is 64 mL. The amount of oxygen evolved was determined by the external standard method.

Isolation of Ru(II)L(pic)(4-HOOC-py) (4-HOOC-py = Pyridine-4-carboxylic Acid). Evaporation of methanol from a solution of complex **1** (0.52 g) in the mixed methanol and water solution gave a dark red precipitate. After filtration and washing with cold ethanol, complex **1** (0.50 g) was obtained as a dark red crystalline solid. The proton NMR spectrum of this solid was identical with the structure of complex **1**. After storage of this solid under aerobic conditions for circa one month, the color of complex **1** was gradually changed from dark red to dark green. This dark green solid was dissolved in methanol, and excess ascorbic acid was added as a reducing agent to convert the solution from green to red. Then, the solvent was evaporated to afford a dark red solid. After purification by column chromatography on silica gel using dichloromethane–methanol (3:4, v/v) as an eluent, Ru(II)L(pic)(4-HOOC-py) was obtained as a dark red solid (0.16 g, 30%). ¹H NMR (400 MHz, CDCl_3): δ 8.60 (d, 2H), 8.04 (d, 2H), 7.92–7.87 (m, 4H), 7.66 (d, 2H), 7.55 (d, 2H), 7.05 (d, 2H), 2.26 (s, 3H). MS (ESI): m/z^+ 605.05 (M + 2Na – H)⁺. Calcd: 605.00. UV–vis, λ_{max} (methanol)/nm: 299 ($\epsilon/\text{dm}^3 \text{ mol}^{-1} \text{ cm}^{-1}$ 22 200), 384 (7800), 460 (5200).

Results and Discussion

Electrochemical Properties. The cyclic voltammogram of complex **1** in a pH 1.0 aqueous solution showed two oxidation waves at 0.86 and 1.11 V, corresponding to the respective $\text{Ru}^{\text{II/III}}$ and $\text{Ru}^{\text{III/IV}}$ processes (Figure 1).⁴⁷ In

(44) Duan, L.; Fischer, A.; Xu, Y.; Sun, L. *J. Am. Chem. Soc.* **2009**, *131*, 10397.

(45) McClenaghan, N. D.; Barigelletti, F.; Mauberta, B.; Campagna, S. *Chem. Commun.* **2002**, 602.

(46) DeSimone, R. E.; Drago, R. S. *J. Am. Chem. Soc.* **1970**, *92*, 2343.

(47) All of the redox potentials reported in this paper are versus NHE. $[\text{Ru}(\text{bpy})_3]^{2+}$ was used as a reference with the $E_{1/2}(\text{Ru}^{\text{II/Ru}^{\text{III}}})$ being 1.26 V versus NHE.

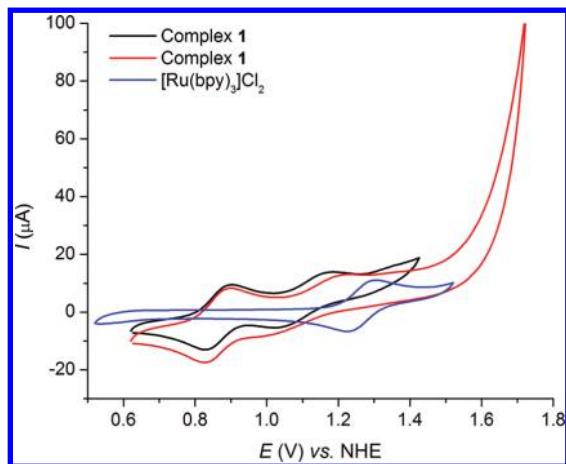


Figure 1. Cyclic voltammograms of **1** (1.0 mM) and $[\text{Ru}(\text{bpy})_3]\text{Cl}_2$ (1.0 mM) in a $\text{CF}_3\text{SO}_3\text{H}$ aqueous solution (pH 1.0) containing 10% acetonitrile.

addition, a catalytic water oxidation peak was observed from 1.5 V. This potential is much higher than the potential of the oxidized state of $[\text{Ru}(\text{bpy})_3]^{2+}$ ($E_{1/2} = 1.26$ V). Consequently, the light-driven water oxidation by complex **1** using $[\text{Ru}(\text{bpy})_3]^{2+}$ as a photosensitizer is thermodynamically unfavored in a pH 1.0 aqueous solution.

Our recent results on the mechanism of water oxidation by complex **1** show that ligand exchange is not necessary and complex **1** can catalyze water oxidation via seven-coordinate ruthenium intermediates.⁴⁴ This type of reaction mechanism was also suggested by Meyer et al. and Thummel et al. recently.^{28,30} Due to this consideration, there is no need to use pH 1.0 conditions for water oxidation if we use an oxidant other than Ce(IV). Therefore, complex **1** could be potentially functional toward water oxidation under neutral conditions. Moreover, water oxidation is favored under less acidic conditions. The electrochemical properties of complex **1** were investigated in the pH 7.0 phosphate buffer solution (Figure 2). A reversible wave is observed at $E_{1/2} = 0.72$ V, which is assigned to the $\text{Ru}^{\text{II/III}}$ process. Further scanning toward the anodic direction results in the catalytic water oxidation curve beginning from ca. 0.98 V, which is ca. 0.5 V lower than that observed in a pH 1.0 aqueous solution. In order to prove that the catalytic curve is indeed due to the catalytic oxidation of water, a reverse scan to -1.0 V was carried out. An irreversible reduction peak at -0.5 V was observed, which was assigned to the reduction of molecular oxygen. In addition, the reversibility of the $\text{Ru}^{\text{II/III}}$ couple suggests that this catalyst has certain stability during the electrochemically catalytic water oxidation. Most importantly, the catalytic potential of complex **1** is 0.28 V lower than the oxidation potential of $[\text{Ru}(\text{bpy})_3]^{2+}$ (Figure 2), which indicates that $[\text{Ru}(\text{bpy})_3]^{3+}$ could drive complex **1** to oxidize water.

Chemical Water Oxidation Driven by $[\text{Ru}(\text{bpy})_3]^{3+}$. Subsequently, chemical water oxidation by catalyst **1** using $[\text{Ru}(\text{bpy})_3]^{3+}$ as the oxidant was investigated. Before the injection of catalyst **1** to the deoxygenated pH 7.0 buffer solution containing $[\text{Ru}(\text{bpy})_3](\text{PF}_6)_3$, oxygen evolution was observed, but with a very low reaction rate, as monitored by Clark-type oxygen electrode (Figure S1,

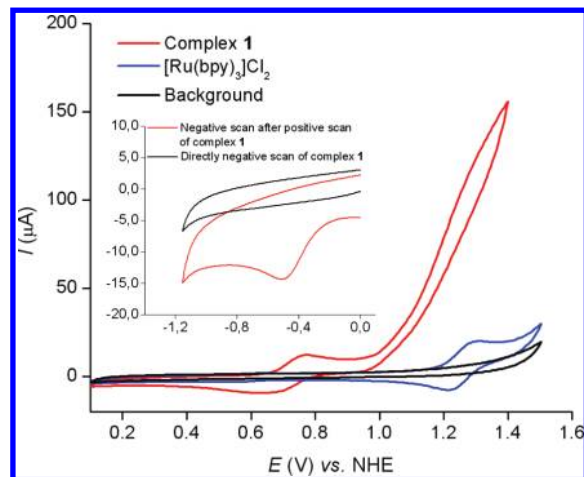


Figure 2. Cyclic voltammograms of **1** (1.0 mM) and $[\text{Ru}(\text{bpy})_3]\text{Cl}_2$ (1.0 mM) as well as the background in a phosphate buffer (pH 7.0, 50 mM) solution containing 10% acetonitrile. The inset shows the reduction peak of generated O_2 and the background.

Supporting Information). In contrast, the injection of catalyst **1** resulted in much faster generation of dioxygen (Figure S1). As expected, complex **1** can function as a water oxidation catalyst by using $[\text{Ru}(\text{bpy})_3]^{3+}$ as a chemical oxidant, indicating that the photogenerated $[\text{Ru}(\text{bpy})_3]^{3+}$ could potentially drive complex **1** to oxidize water.

Photochemical Water Oxidation: Oxygen Formation Measured in Liquid Phase. To construct an artificial system that drives water oxidation with visible light, we employed a three-component system composed of $[\text{Ru}(\text{bpy})_3]\text{Cl}_2$ as a photosensitizer, $[\text{Co}(\text{NH}_3)_5\text{Cl}]\text{Cl}_2$ as a sacrificial electron acceptor, and complex **1** as a catalyst (Scheme 1). $[\text{Co}(\text{NH}_3)_5\text{Cl}]^{2+}$ reacts with the excited ruthenium complex, $[\text{Ru}(\text{bpy})_3]^{2+*}$, to generate the $[\text{Ru}(\text{bpy})_3]^{3+}$ species (eq 1).^{48,49}

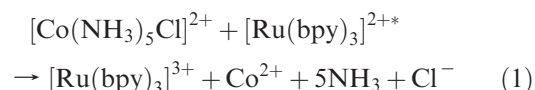


Figure 3 depicts the photochemical water oxidation monitored by the Clark-type oxygen electrode. In the absence of light, as complex **1** was added into the deoxygenated phosphate buffer (pH 7.0) solution containing $[\text{Co}(\text{NH}_3)_5\text{Cl}]\text{Cl}_2$ and $[\text{Ru}(\text{bpy})_3]\text{Cl}_2$, no oxygen was formed. Irradiation of the above solution immediately resulted in the evolution of dioxygen, and its concentration reached a highest value of ca. 390 nmol after 7 min (Figure 3, curve c). The deactivation of this system was due to the decomposition of the photosensitizer while most of complex **1** was also decomposed. From the slope of the initial oxygen evolution, the maximum turnover frequency (TOF_{max}) for catalyst **1** was found to be $> 550 \text{ h}^{-1}$ (see Figure S2, Supporting Information). The final pH after the illumination was tested to be 7.7, which is due to the release of NH_3 according to eq 1.

To prove that the oxygen generated in the above reaction was indeed promoted by catalyst **1**, several control experiments were conducted: (1) Under the same conditions but without the photosensitizer, no oxygen

(48) Gafney, H. D.; Adamson, A. W. *J. Am. Chem. Soc.* **1972**, *94*, 8238.
(49) Navon, G.; Sutin, N. *Inorg. Chem.* **1974**, *13*, 2159.

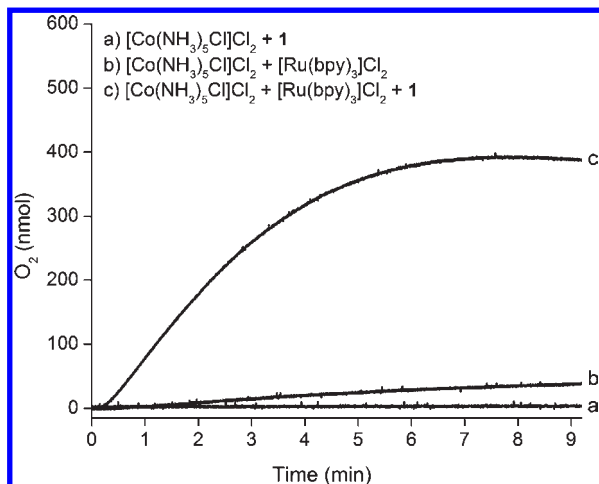


Figure 3. Photochemical oxygen evolution in 2 mL phosphate buffer (initial pH 7.0, 50 mM) solutions of (1) $[\text{Co}(\text{NH}_3)_5\text{Cl}]\text{Cl}_2$ (2.9×10^{-2} M) + **1** (5.5×10^{-6} M), curve a; (2) $[\text{Co}(\text{NH}_3)_5\text{Cl}]\text{Cl}_2$ (2.9×10^{-2} M) + $[\text{Ru}(\text{bpy})_3]\text{Cl}_2$ (6.7×10^{-5} M), curve b; (3) $[\text{Co}(\text{NH}_3)_5\text{Cl}]\text{Cl}_2$ (2.9×10^{-2} M) + $[\text{Ru}(\text{bpy})_3]\text{Cl}_2$ (6.7×10^{-5} M) + **1** (5.5×10^{-6} M), curve c.

was generated in the presence of light (Figure 3, curve a), showing that $[\text{Ru}(\text{bpy})_3]^{2+}$ is necessary for water oxidation in this three-component system. (2) Without catalyst **1**, the system of $[\text{Co}(\text{NH}_3)_5\text{Cl}]\text{Cl}_2$ and $[\text{Ru}(\text{bpy})_3]\text{Cl}_2$ in a phosphate buffer (pH 7.0) could also produce dioxygen under irradiation (Figure 3, curve b). However, the oxygen evolution rate is much slower than that of the three-component system, confirming that catalyst **1** is indeed involved in the catalytic water oxidation processes. (3) Although the cobalt ion was reported to catalytically oxidize water and the $[\text{Co}(\text{NH}_3)_5\text{Cl}]\text{Cl}_2$ in our system can be reduced to form Co^{2+} during the photochemical reaction (eq 1), no obvious promotion on oxygen evolution was observed in our triad system using $\text{Co}(\text{OAc})_2$ (5.5×10^{-6} M and 1.25×10^{-4} M) instead of complex **1** (5.5×10^{-6} M), indicating that the catalytic water oxidation by the cobalt ion is negligible if any. (4) When RuCl_3 and $\text{Ru}(\text{bpy})_2\text{Cl}_2$ were used instead of catalyst **1**, no obvious promotion of oxygen was observed compared with the system containing $[\text{Co}(\text{NH}_3)_5\text{Cl}]\text{Cl}_2$ and $[\text{Ru}(\text{bpy})_3]\text{Cl}_2$. (5) A light control experiment shows that the catalytic water oxidation in the system is driven by light (Figure 4). All of these results clearly confirmed the light-driven water oxidation by the molecular catalyst **1**.

Another commonly used electron acceptor, $\text{Na}_2\text{S}_2\text{O}_8$, was also investigated in the typical three-component system. $\text{S}_2\text{O}_8^{2-}$ is known to react with $[\text{Ru}(\text{bpy})_3]^{2+}$ to form $[\text{Ru}(\text{bpy})_3]^{3+}$ following an oxidative quenching reaction (eq 2) and a thermal reaction (eq 3).⁵⁰

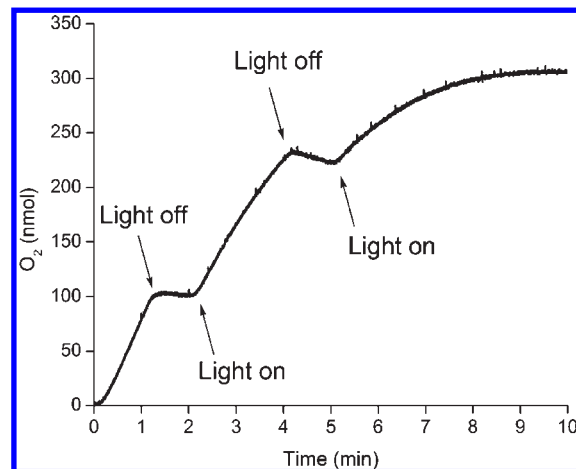
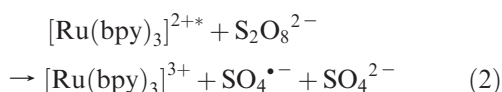


Figure 4. Light control experiment of the photochemical water oxidation in a 2 mL phosphate buffer (initial pH 7.0, 50 mM) solution of $[\text{Co}(\text{NH}_3)_5\text{Cl}]\text{Cl}_2$ (2.9×10^{-2} M), $[\text{Ru}(\text{bpy})_3]\text{Cl}_2$ (6.7×10^{-5} M), and **1** (5.5×10^{-6} M).

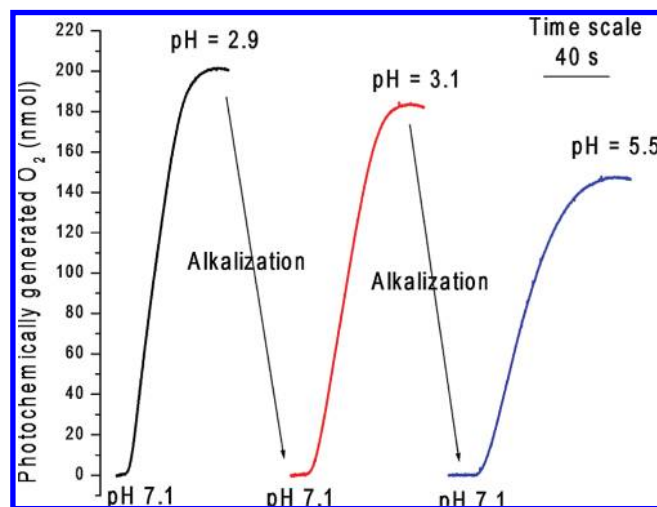


Figure 5. Illustration of the repetitive reactivation of a photochemical water oxidation system. The reaction system is a 2 mL phosphate buffer (initial 7.2, 8.3 mM) solution of $\text{Na}_2\text{S}_2\text{O}_8$ (1×10^{-2} M) + $[\text{Ru}(\text{bpy})_3]\text{Cl}_2$ (1×10^{-3} M) + **1** (9.5×10^{-6} M). A sodium hydroxide aqueous solution (0.3 M) was used for the alkalization.

It was found that the pH value of the fresh solution of sodium persulfate (10 mM) in a phosphate buffer (initial pH 7.2) is actually 7.1 at 23 °C; so the addition of sodium persulfate to a pH 7.2 buffer will increase the acidity. The photochemical water oxidation was conducted under the given conditions in Figure 5. Molecular oxygen was generated quickly under irradiation, and the TOF_{max} of complex **1** was calculated to be $> 1250 \text{ h}^{-1}$ (see Figure S3, Supporting Information). The lifetime of this three-component system was shortened to ca. 50 s in comparison to 7 min for the triad system using $[\text{Co}(\text{NH}_3)_5\text{Cl}]^{2+}$ as the electron acceptor. When the formation of dioxygen stopped, the pH value of the solution dropped to 2.9 from 7.1. According to the CV studies of complex **1** in an aqueous solution, its catalytic properties are sensitive to the acidity of aqueous solution. An increase of acidity could shift the onset potential of the catalytic curve to a positive direction. Thus, the catalytic activity would be decreased upon increasing the acidity of the solution,

(50) Henbest, K.; Douglas, P.; Garley, M. S.; Mills, A. J. *Photochem. Photobiol. A: Chem.* **1994**, *80*, 299.

which might be the reason of the deactivation of our photochemical oxygen evolution system.

To confirm this presumption, the deactivated solution (pH 2.9) was neutralized to 7.1 with a sodium hydroxide aqueous solution and irradiated again. Apparently, rapid oxygen formation was observed (Figure 5), indicating that the deactivation is due to the increase of the acidity. After the second run, the final pH dropped to 3.1. Repeated neutralization could regenerate the activity once again. After the third run of the photochemical water oxidation, the pH value decreased to 5.5. During these repetitive experiments, the amount of oxygen formed in each run decreased gradually. After the third run, the addition of more $\text{Na}_2\text{S}_2\text{O}_8$ to the deactivated system followed by neutralization, however, could restore the catalytic activity as good as the first run, implying that the catalyst is rather stable under the given conditions. Compared with $\text{S}_2\text{O}_8^{2-}$, $[\text{Co}(\text{NH}_3)_5\text{Cl}]^{2+}$ releases NH_3 molecules after its decomposition that react with the released protons during the photochemical water oxidation and buffer the catalytic system. Therefore, we prefer to use $[\text{Co}(\text{NH}_3)_5\text{Cl}]^{2+}$ as the sacrificial electron acceptor instead of $\text{S}_2\text{O}_8^{2-}$ in the following measurements.

According to the electrochemical data of complex **1**, it is possible to use another photosensitizer which has a milder oxidation potential than $[\text{Ru}(\text{bpy})_3]^{2+}$ to drive complex **1** to oxidize water. To investigate this possibility, an electron richer ruthenium complex $[\text{Ru}(\text{dmbpy})_3](\text{PF}_6)_2$ with $E_{1/2}(\text{Ru}^{\text{II/III}}) = 1.10$ V which is 0.16 V lower than that of $[\text{Ru}(\text{bpy})_3]^{2+}$, was used as the photosensitizer. Interestingly, no oxygen was observed upon the irradiation of the mixture containing $[\text{Ru}(\text{dmbpy})_3]^{2+}$ and $[\text{Co}(\text{NH}_3)_5\text{Cl}]\text{Cl}_2$ in pH 7.0 phosphate buffer (Figure S4). $\text{Co}(\text{OAc})_2$ was used once again to test its catalytic ability and no obvious oxygen generation was detectable in the system. Only if catalyst **1** was included in the system, O_2 evolution could be detected under illumination (Figure S4). Apparently, it is catalyst **1** that promotes water oxidation in this system. The rate of the oxygen generation ($\text{TOF}_{\text{max}} = 360$, see Figure S5) is lower than that of the system with $[\text{Ru}(\text{bpy})_3]^{2+}$, due to the smaller driving force from $[\text{Ru}(\text{dmbpy})_3]^{3+}$ for water oxidation. Nevertheless, light-driven water oxidation using $[\text{Ru}(\text{dmbpy})_3]^{2+}$ as a photosensitizer has not been reported before because of the milder oxidation ability of $[\text{Ru}(\text{dmbpy})_3]^{2+}$ and the lack of a proper water oxidation catalyst bearing such a low overpotential. Concerning these aspects, complex **1** is a promising catalyst that promotes water oxidation at such a low oxidation potential.

Photochemical Water Oxidation: Oxygen Formation Measured in the Gas Phase. The light-driven catalytic water oxidation in our three-component system with $[\text{Ru}(\text{bpy})_3]^{2+}$ as the sensitizer has been further confirmed by the detection of O_2 in the gas phase above the reaction solution with GC (Figure 6). Photochemically generated oxygen in the system without catalyst **1** was too little to be detected by GC under our conditions. In contrast, the system including catalyst **1** led to fast oxygen evolution upon irradiation. Under the given conditions in Figure 6, the evolved oxygen reached a maximum of $4.96 \mu\text{mol}$ after 2 h of irradiation, and the relative turnover number

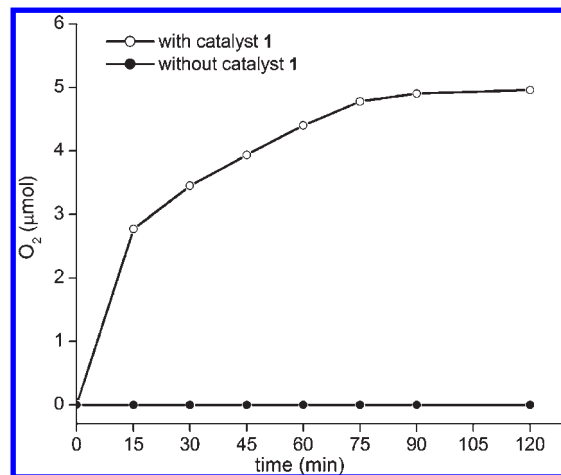


Figure 6. Photochemical water oxidation monitored by GC. The reaction systems are 5 mL phosphate buffer (pH 7.0, 50 mM) solutions of (1) $[\text{Co}(\text{NH}_3)_5\text{Cl}]\text{Cl}_2$ (2.9×10^{-2} M) + $[\text{Ru}(\text{bpy})_3]\text{Cl}_2$ (1×10^{-5} M), ●; (2) $[\text{Co}(\text{NH}_3)_5\text{Cl}]\text{Cl}_2$ (2.9×10^{-2} M) + $[\text{Ru}(\text{bpy})_3]\text{Cl}_2$ (1×10^{-5} M) + **1** (1×10^{-5} M), ○.

was calculated to be ca. 100 for both catalyst **1** and $[\text{Ru}(\text{bpy})_3]^{2+}$.

Decomposition of Complex 1 in Acetonitrile and the Solid State: Aerobic Oxidation of the sp^3 C–H Bond. Complex **1** could be gradually oxidized under aerobic conditions not only in solution but also in the solid state. The solution of complex **1** in acetonitrile was stirred at room temperature under an air atmosphere for one day, during which the color of the above solution changed gradually from red to green. The final solution was analyzed by ESI mass spectrometry in positive mode. The spectrum of the above green solution shows three main peaks in the 500–600 region, at $m/z^+ = 530.07$, 559.07, and 581.05, respectively, assigned to the monocationic species $[\text{Ru}(\text{II})\text{L}(\text{pic})_2]^+$, $[\text{Ru}(\text{II})\text{L}(4\text{-HCO-py})_2 + \text{H}]^+$ (calcd: $m/z^+ = 559.02$) and $[\text{Ru}(\text{II})\text{L}(4\text{-HCO-py})_2 + \text{Na}]^+$ (calcd: $m/z^+ = 581.00$) (see Figure S6, Supporting Information; 4-HCO-py = 4-pyridinecarboxaldehyde). The assignment of the $\text{Ru}(\text{II})\text{L}(4\text{-HCO-py})_2$ species was according to the isolation of $\text{Ru}(\text{II})\text{L}(\text{pic})(4\text{-HOOC-py})$ from the degradation products of complex **1** in the solid state (see structures in Figure 7).

Recrystallization of complex **1** from the mixture of methanol and water afforded a dark red precipitate whose ^1H NMR spectrum is identical with the structure of complex **1**. During the storage of this precipitate under aerobic conditions for about one month, the color of the precipitate changed from dark red to dark green. Dissolution of the dark green solid gave a green solution, to which excess ascorbic acid was added to reduce the high valent ruthenium complexes, resulting in the formation of a red solution. From this solution, one main degradation product was isolated as $\text{Ru}(\text{II})\text{L}(\text{pic})(4\text{-HCOO-py})$, which was characterized by ^1H NMR spectroscopy and MS spectrometry (see spectra in Figure S7, Supporting Information). For the ^1H NMR spectrum of this complex in methanol- d_4 , there are seven peaks in the aromatic region corresponding to 14 protons and one singlet at 2.26 ppm corresponding to 3 protons, assigned to the aromatic protons and methyl protons of 4-picoline, respectively. The MS peak at $m/z^+ = 605.05$ was assigned to

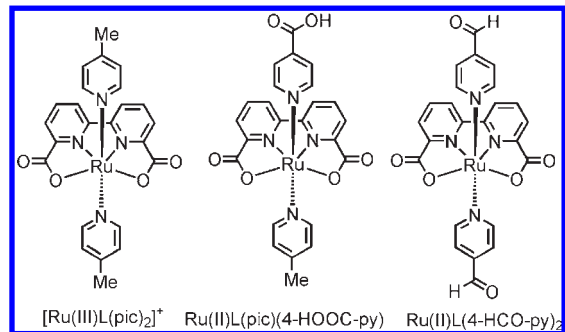


Figure 7. Structures of $[\text{Ru}(\text{III})\text{L}(\text{pic})_2]^+$, $\text{Ru}(\text{II})\text{L}(\text{pic})(4\text{-HOOC-py})$, and $\text{Ru}(\text{II})\text{L}(\text{pic})(4\text{-HCOO-py})$.

$[\text{Ru}(\text{II})\text{L}(\text{pic})(4\text{-HOOC-py}) + 2\text{Na} - \text{H}]^+$ (calcd: 605.00). Concerning the isolation of $\text{Ru}(\text{II})\text{L}(\text{pic})(4\text{-HCOO-py})$, some highly oxidizing ruthenium derivatives from complex **1** under aerobic conditions were formed and could promote aerobic oxidation of the sp^3 C–H bond. Although $\text{Ru}(\text{II})\text{L}(\text{pic})(4\text{-HCOO-py})$ could still catalyze water oxidation using $\text{Ce}(\text{IV})$ under pH 1.0 conditions, it indicates that one of the degradation pathways of our catalyst under catalytic conditions might be the degradation of ligands because at least the $\text{Ru}(\text{IV})$ species, a highly oxidizing species, is present in our catalytic system in order to oxidize water.

Photostability of Complex 1. The photostability of complex **1** is of importance in light-driven water oxidation. Monodentate ligand photodissociation from ruthenium complexes is known. Typically, photoinduced dissociation of 4-aminopyridine from ruthenium complexes has been reported in several cases.^{51,52} Therefore, the photostability of complex **1** is needed to be established. Photodissociation of **1** in a pH 7.0 phosphate buffer containing 5% acetonitrile was studied by UV–vis spectroscopy. After 2 h of irradiation of the above solution, no decomposition of complex **1** was detectable by UV–vis (Figure 8), indicating that complex **1** is very stable in the presence of light. Although the photostability of the higher valent Ru species is not demonstrated, the present observations including the degradation of **1** in the solid state and the good photostability of $\text{Ru}(\text{II})$ species convince us to believe that the deactivation of our system is due to the oxidative degradation of organic ligands rather than the photodecomposition.

Conclusions

The pH-dependent catalytic properties of complex $\text{Ru}(\text{II})\text{L}(\text{pic})_2$ (**1**) toward water oxidation was studied by electrochemistry, showing that complex **1** could electrochemically catalyze water oxidation at relatively low potentials in a pH 7.0 phosphate buffer. Such a low potential allows us to

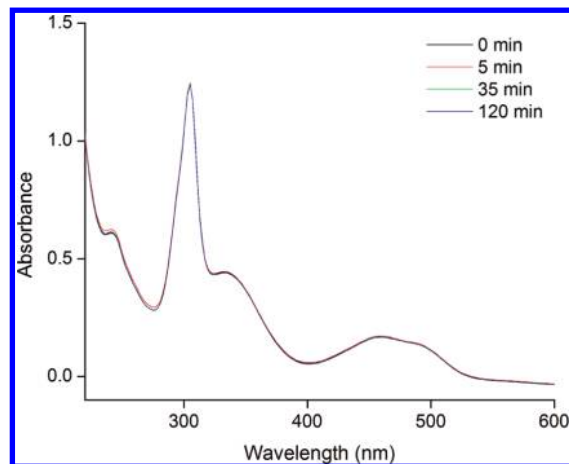


Figure 8. Absorbance-time traces of 5×10^{-5} M complex **1** in a phosphate buffer (pH 7.0) containing 5% acetonitrile upon visible light irradiation.

use $[\text{Ru}(\text{bpy})_3]^{2+}$ and even $[\text{Ru}(\text{dmbpy})_3]^{2+}$ to serve as a photosensitizer to drive complex **1** to oxidize water. Consequently, visible-light-driven water oxidation was demonstrated in a three-component system containing $[\text{Ru}(\text{bpy})_3]^{2+}$ or $[\text{Ru}(\text{dmbpy})_3]^{2+}$ as a photosensitizer, $[\text{Co}(\text{NH}_3)_5\text{Cl}]^{2+}$ or $\text{S}_2\text{O}_8^{2-}$ as a sacrificial electron acceptor, and complex **1** as a water oxidation catalyst. Furthermore, the high photostability of complex **1** was established by photolysis measurements under the same light source as in the photochemical water oxidation reactions. In addition, the aerobic sp^3 C–H bond activation of the pic ligand in complex **1** was observed in both solution and the solid state, indicating that highly oxidizing species were generated. Accordingly, the rapid degradation of complex **1** in the catalytic cycles might be caused by some highly oxidizing intermediates via ligand oxidation instead of photodissociation. The detailed mechanism of photoinduced water oxidation by **1** is under investigation, and structural modification on complex **1** to produce catalysts with even lower overpotentials and higher stability toward water oxidation is also in progress.

Acknowledgment. We acknowledge the Swedish Research Council, K & A Wallenberg Foundation, the Swedish Energy Agency, China Scholarship Council (CSC), National Natural Science Foundation of China (20633020), National Basic Research Program of China (2009CB220009), and the Program for Changjiang Scholars and Innovative Research Team in University (IRT0711) for financial support of this work.

Note Added after ASAP Publication. This paper was published on the Web on December 8, 2009, with a minor error in equation 2. The corrected version was reposted on December 28, 2009.

(51) Salassa, L.; Garino, C.; Salassa, G.; Nervi, C.; Gobetto, R.; Lamberti, C.; Gianolio, D.; Bizzarri, R.; Sadler, P. J. *Inorg. Chem.* **2009**, *48*, 1469.

(52) Zayat, L.; Calero, C.; Albores, P.; Baraldo, L.; Etchenique, R. *J. Am. Chem. Soc.* **2003**, *125*, 882.

Supporting Information Available: Figures S1–S7. This material is available free of charge via the Internet at <http://pubs.acs.org>.